International Journal of Geology, Earth & Environmental Sciences ISSN: 2277-2081
An Open Access, Online International Journal Available at http://www.cibtech.org/jgee.htm
2026 Vol. 16, pp. 1-16/Karl
Research Article

SURFACE CHANGES OF THE WESTERN ALBORAN GYRE

***Karl Heinz Szekielda**
Fulbright Alumnus
University of The Bahamas, The Bahamas
Ateneo de Manila University, Philippines
**Author for Correspondence: kszekielda@ateneo.edu*

ABSTRACT
The research evaluates observations of the Western Alboran gyre at various time-scales to describe changes of temperature and chlorophyll concentration with monthly time series. Averaged and seasonal conditions show that the western gyre is positioned more or less in the center of the Alboran Sea, but temperature distribution shows maximum temperatures >19.5^{0}C, closer towards the north African coast. The Atlantic Jet carries temperatures at <19^{0}C through the Strait of Gibraltar, and upwelling water is added to the jet from the Spanish coast into the outer periphery of the western gyre. The average concentrations of chlorophyll are less than 0.3 mg m^{-3} for the incoming water from the Atlantic Ocean through the Strait of Gibraltar, but in the upwelling region along the Spanish Coast, chlorophyll concentrations are greater than 1 mg m^{-3}.
The central part of the gyre is characterized by concentrations of less than 0.4 mg m^{-3}, but concentrations are higher compared to those of the incoming Atlantic water. Averaged yearly means reveal the prevailing influence of the Atlantic Jet on temperature and chlorophyll distribution especially at the outer periphery of the gyre. The comparison of temperature and chlorophyll distributions show that the jet is also partly acting as a transport system for elevated chlorophyll concentrations in patches that are generated in the northern coastal upwelling. Short-term fluctuations of chlorophyll concentrations are identified in regions where patch generation was realized. The chlorophyll data indicate that patch generation is mostly a seasonal effect and was shown with Hovmöller latitude averaged analysis. Patches related to blooming events appear within a few days, but there is not always a continuous transport of upwelled water into the outer ring, and the chlorophyll gradients are not always in sync with those of temperature. On average, about every twenty days, a blooming event may occur in response to upwelling, and chlorophyll patches at the outer ring can move at a surface velocity of about 0.3 to 0.5 cm sec^{-1}. The western gyre may change its circulation from an anticyclonic to cyclonic mode within eighteen days and this short period adds to the complicated surface distribution of chlorophyll.

Keywords: *Western Alboran Sea, Gyres, Chlorophyll, Geostrophic Surface Currents*

INTRODUCTION
The Mediterranean Sea is a semi-enclosed basin where evaporation exceeds precipitation, and, as a result, the deficit is balanced by an inflow of Atlantic surface water through the Strait of Gibraltar to the Alboran Sea. Zonal atmospheric circulation in the vicinity of the Strait shows significant covariance with the inflow and outflow through the strait, and anomalously fluxes have a strong impact on the Alboran Sea's ecosystem (Boutov *et al.,* 2014). The Atlantic water and water from the Alboran Sea develop eddy formation and strong frontogenesis. The incoming Atlantic Water to the Mediterranean Sea builds in the Alboran Sea two major anticyclonic gyres that are referred to as the Western and Eastern Alboran gyres (Parrilla, and Kinder, 1984). This circulation scheme has been identified earlier through satellite observations (LaViolette, 1984), and large variations were found in the surface expression of these two gyres that are further extended by fluctuations in the intensity of water exchange through the Strait of Gibraltar, coastal upwelling, internal waves, development of density fronts and strong meso- and sub-mesoscale turbulence (Esposito *et al.,* 2021).

The incoming Atlantic water forms the Atlantic Jet that is intensified by wind-driven surface transport and surrounds both the anticyclonic Western Alboran Gyre and the Eastern Alboran Gyre (Oguz *et al.,* 2014). The western part of the jet has a diameter of about 100 to 150 km and is located roughly between the Strait of Gibraltar and the northwestern sector of the basin (Sarhan *et al.,* 2000). The jet carries a lower salinity than the surrounding water and moves at a velocity of about 1 m s^{-1} (Parrilla and Kinder, 1987). Whereas the Atlantic jet seems to be the main driver for larger scale propagation (Maćis *et al.,* 2007), zonal winds are also forcing factors in changing the intensity and location of the surface currents. The jet undergoes seasonal variations through interaction with the Western Alboran Gyre and a cyclonic eddy that develops in the north close to the Spanish coast (Brett *et al.,* 2020; Sanchez-Garrido *et al.,* 2013; Renault *et al.,* 2012; Moran and Estrada, 2001). This cyclonic eddy may partially block the flux of surface water from the Strait of Gibraltar and is more pronounced during the winter seasons due to meteorological enhancement. The variability of the jet also affects the upwelling region in the Alboran Sea, in particular, at the northwestern edge in the presence of westerly winds from the Spanish coast, and is responsible for increased primary production and sporadic blooming events (Capó *et al.,* 2021; Reul et al.,2015). In response to seasonal changes, the jet changes its velocity and direction with a stronger flow towards the northeast during the first half of the year, but a weaker flow is observed at the end of the year (Maćias *et al.,* 2016). The flow through the Strait of Gibraltar is also impacted by tides and the topography of the Strait of Gibraltar (LaViolette and Lacombe, 1988). During flood, the tide has a westward flow, but an eastward propagating internal tidal bore can evolve into a packet of solitary internal waves (Capó *et al.,* 2021).

As a result, an enlarged pool of mixed water is formed in the basin (Garcıá-Lafuente *et al.,* 2013), and this mixing has an important impact on the nutrient budget because the Atlantic Jet delivers additional nutrients to the euphotic zone (Maciás *et al.,* 2009; Huertas *et al.,* 2012; Sánchez Garrido *et al.,* 2015). Furthermore, the nutrient budget in the Western Alboran Sea is also regulated by wind-driven upwelling that prevails mainly in the coastal shelf region, whereas offshore upwelling is linked to the change in the position of the Atlantic Jet and its flow around the anticyclonic western gyre (Macías *et al.,* 2007).

Prevailing winds in the Alboran Sea are the easterly winds (Levantis) and westerly winds (Ponientes), where the latter is common during winter and spring and produce a cooling of the sea surface due to upwelling between Estepona and Malaga, whereas the Levantes blows from the east and appears during the dry season (Parrilla and Kinder, 1987). The cold surface water in the northern edge of the Atlantic Jet forms a sharp density front (Sarhan *et al.,* 2000; Cheney and Doblar, 1982), and frontogenesis with large vertical velocities are observed in the vicinity of the jet at a velocity of about 30 m d^{-1}. Enhanced primary productivity is the consequence, and phytoplankton patches are disseminated within the basin by mesoscale eddies that can create chaotic flow at the periphery of the Western Alboran gyre (Oguz *et al.,* 2014). Frontogenesis is especially present in the easternmost region during the cold season when the surface flow is strongly influenced by the intrusion of the salty Northern Current (Capó *et al.,* 2021). Wind-induced upwelling is mainly on the northern side of the gyre off the Spanish coast, whereas gyre-induced upwelling is generated at the periphery of the gyre (Bárcena *et al.,* 2004; Garćıa-Gorriz and Carr, 2001). Ramírez *et al.* (2021) pointed out that elevated chlorophyll concentrations at the periphery of the gyre are effects of an uplifted pycnocline, whereas the inner part of the Western Alboran Gyre is characterized by a depressed pycnocline that parallels a depressed nutricline within the gyre at about 70 to 115 m (Moran and Estrada, 2001). Extremely high primary production is reported in the frontal system between the Western Alboran Gyre and the Atlantic Jet, at average values of ~ 632 mg C m^{-2} d^{-1} while the minimum in the center of the gyre is around 330 mg C m^{-2} d^{-1} (Moran and Estrada, 2001). The cyclonic region between the western and eastern anticyclonic gyres shows an uplifted pycnocline due to upwelling (Vargas-Yáñez *et al.,* 2021; Sánchez-Garrido and Nadal, 2022), whereas the centers of the two anticyclonic gyres are characterized by low concentrations of chlorophyll, because their nutricline is located at depths of about 70 to 115 m (Moran and Estrada, 2001). The seasons in the Alboran Sea show major bloom conditions from November to March, and the summer is considered as a non-bloom regime

that is observed from May to September. In addition, two transition periods appear from April to May when thermal stratification starts. A second transition period is observed from October–November when vertical stratification of the water column is reduced (Garćıa-Gorriz and Carr, 2001).

It can be postulated that the western Alboran Sea is also a region where the effect of global change may be enhanced, because of the many varying processes that determine the physical and biological conditions. In particular, global warming may affect the marine ecosystem and therefore it is important to interpret all present available data sets in order to establish a baseline for assessing anticipated future anomalies and environmental damage (Cherif *et al.,* 2020). In this context, the following research has the objective to document with satellite-derived data observed changes in the western Alboran Sea with focus on the Western Alboran Gyer. This gyre is located in the region where the primary interaction of the incoming Atlantic Jet with the Alboran water takes place before it continues its path towards the Eastern Anticyclonic gyre.

The processes in the Alboran Sea appear at various times and space scales and therefore, the study presents the interpretation of data at various temporal resolutions with data that cover a time span of roughly two decades. The first section in this study deals at low temporal and spatial resolution with average maps of sea surface temperature and chlorophyll concentrations with a description of seasonal changes that is based on monthly resolution of time series of temperature and chlorophyll. Details at higher temporal resolutions were extracted from data that were collected in 2024 and 2025 and describe short-term fluctuations in regions where patch generation was detected. In the final section, an overall conclusion from the analyzed data will be presented.

MATERIALS, METHODS AND DESCRIPTION OF THE ANALYZED REGION

The temperature, chlorophyll and wind data were processed with Giovanni, a system for multidisciplinary research and applications (Acker and Leptoukh, 2007). Sea surface temperature at 4km-resolution was retrieved from Aqua MODIS Global Mapped C1615905770-OB_DAACVersion R2019.0. Additional image material was extracted from NASA's EOSDIS through <https://worldview.earthdata.nasa.gov>. Supplementary chlorophyll images were derived from the European Space Agency's Ocean Virtual Laboratory (https://ovl.oceandatalab.com/) product [Chl-a (oc4me)OLCL Sentinel-3 (ESA, ODL)]. Corresponding geostrophic surface streamlines (Globcurrent, CMEMS) were also retrieved from the Ocean Virtual Laboratory that provides zonal and meridional velocities mapped at 1/4 degree.

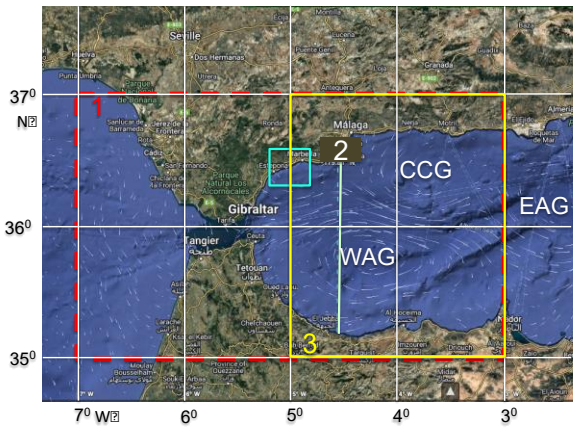

Figure 1: The region of observations showing the sites of investigations with the major surface streamlines. WAG, Western Anticyclonic Gyre; EAG, Eastern Anticyclonic Gyre; CCG, Central Cyclonic Gyre.

The research focused on various sites that are shown in Figure 1, and addressed specific tasks. Data in Site 1 were used for describing the general climatic surface conditions in the site with temperature and chlorophyll distribution. Site 2 covers a narrow strip at $4^0$36'W, $35^0$15'N to 4^0 30'W, $36^0$45'N, that starts at the southern coast of Spain with its upwelling system, crosses the Atlantic Jet, leads through the center of the gyre and ends at the African coast. The yellow rectangle 3 marks the region where the Western Alboran Gyre is located most of the year and where major surface changes can be expected. The green square, close to the Spanish coast, defines the area for which wind data were analyzed.

RESULTS

Climatology and seasonal changes

The climatological data in Figure 2 give the average conditions for surface currents, sea surface temperature and chlorophyll concentrations that were averaged over a period from 2002 to 2025. Figure 2A shows the generalized surface circulation in the vicinity of the Alboran Sea that includes the Atlantic Jet starting at the Strait of Gibraltar, the western and eastern anticyclonic Alboran gyres, the central cyclonic gyre and the Almeria-Oran front. Figures 2B and 2C focus on the region of the western Alboran gyre with averaged temperature and chlorophyll distributions. The surface circulation shows that the western gyre is positioned at the center of the Alboran Sea although the temperature distribution shows a maximum of >19.5^{0}C towards the North African coast. This indicates the cooling effect of the Atlantic Jet in the north that carries temperatures at <19^{0}C through the Strait of Gibraltar and receives an additional contribution of cold upwelled water from the Spanish coast.

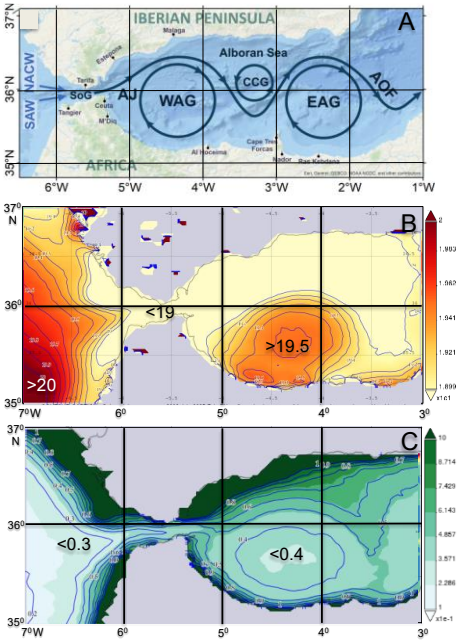

Figure 2: Average state of the Alboran Sea. A: Schematic of the general surface circulation in the vicinity of the Alboran Sea showing the Atlantic Jet (AJ), the Western and Eastern Alboran Gyres (WAG and EAG), the Central Cyclonic Gyre (CCG), and the Almeria-Oran front (AOF) (adapted from Sánchez-Garrido and Nadal, 2022). Figures B and C give the averaged distribution of sea surface temperature (^{0}C) and chlorophyll (mg m^{-3}) concentrations, respectively, for 2002 to 2025, in the region of the Western Alboran Gyre, and are generated with GIOVANNI.

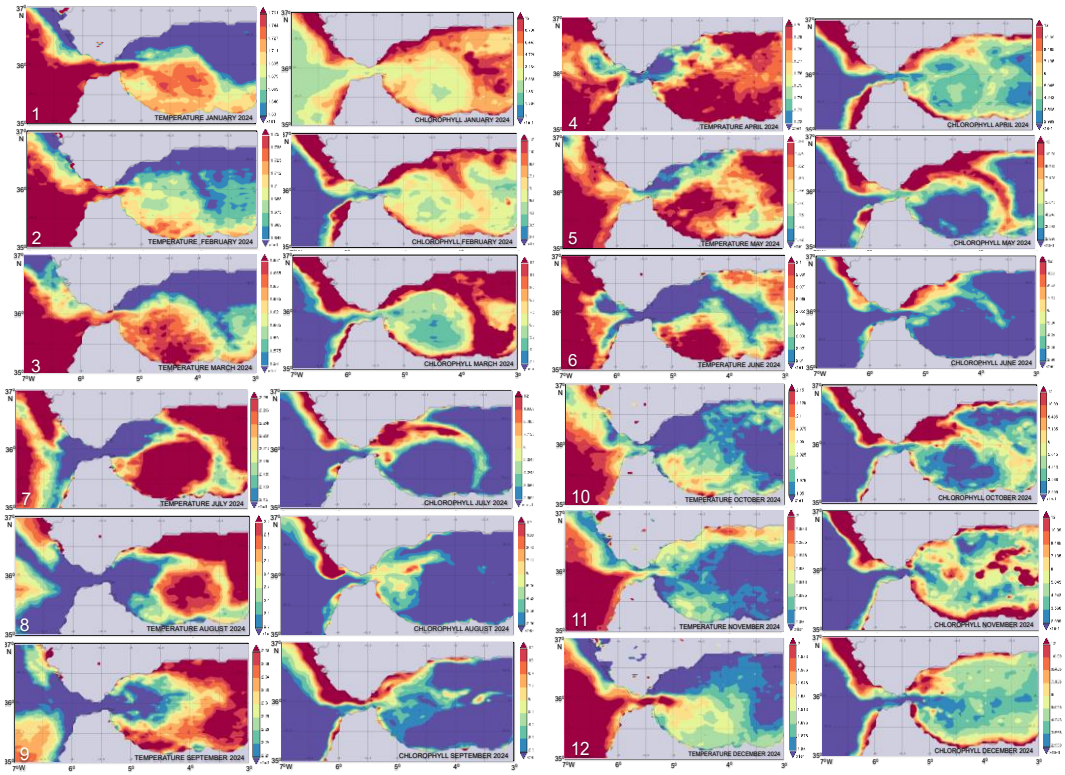

Figure 3: Monthly averaged surface temperature (^{0}C) and chlorophyll concentrations (mg m^{-3}) for January to December 2024. The numbers in the lower left corners refer to the corresponding months. The color annotations to temperature values have been adjusted according to the apparent temperature range in a specific month, but the chlorophyll images have all the same range of color annotations throughout the year. The investigated region is shown in Figure 1 and is outlined as a red rectangle 1, covering 7^{0}W, 35^{0}N to 3^{0}W, 37^{0}N.

The high chlorophyll concentrations in the northern part of the Alboran Sea are the result of coastal upwelling and transport of elevated chlorophyll concentrations from the upwelling region into the outer part of the gyre. The central part of the gyre is characterized by low chlorophyll concentrations of <0.4 mg m^{-3}, but the concentrations are still higher compared to those of the incoming Atlantic water that has less than 0.3 mg m^{-3}. The patterns in the distribution of temperature and chlorophyll are similar despite the fact that the biological response to physical processes would be a factor leading to heterogeneity.

Monthly changes

Seasonal mapping based on averaged data over two decades suppresses emerging short-time changes of the gyre, but monthly averaged data provide more details as shown in Figure 3. From January to March, warm Atlantic water enters the western Alboran Sea, and during this period, the center of the gyre has the lowest concentrations of chlorophyll, although cold water from the upwelling region along the Spanish coast is transported along the outer periphery of the gyre, and blooming is recognized by the high chlorophyll concentrations.

By March, the cold water extends farther south, and maximum concentrations of chlorophyll are found close to the African continent. By April-May, the gyre is less recognized by surface temperature, but by July/August, the heat accumulation in the gyre's center creates a strong thermal gradient that makes the

gyre a distinct feature. The chlorophyll concentrations are elevated for the period January to July in the upwelling region, and high concentrations appear along the eastern side of the gyre. However, in July/August, the center shows decreasing concentrations that coincides with increasing surface temperature in the center.

From October to December, chlorophyll concentrations and temperature indicate a weakening of the gyre that is connected to changes of Atlantic water transported through the Strait of Gibraltar due to meteorological forcing (Vargas-Yáñez *et al.,* 2002; Vélez-Belchí *et al.,* 2005). For the rest of the year, the thermal monthly data show weak boundaries of the gyre and is the result of fluctuations in the position of the gyre.

A general presentation of seasonal changes in the region of the western anticyclonic gyre is shown in Figure 4 with the Hovmöller analysis of latitude-averaged chlorophyll concentrations. The distribution shows that elevated chlorophyll concentrations appear in distinct patches with a seasonal appearance from February to March and from October to November.

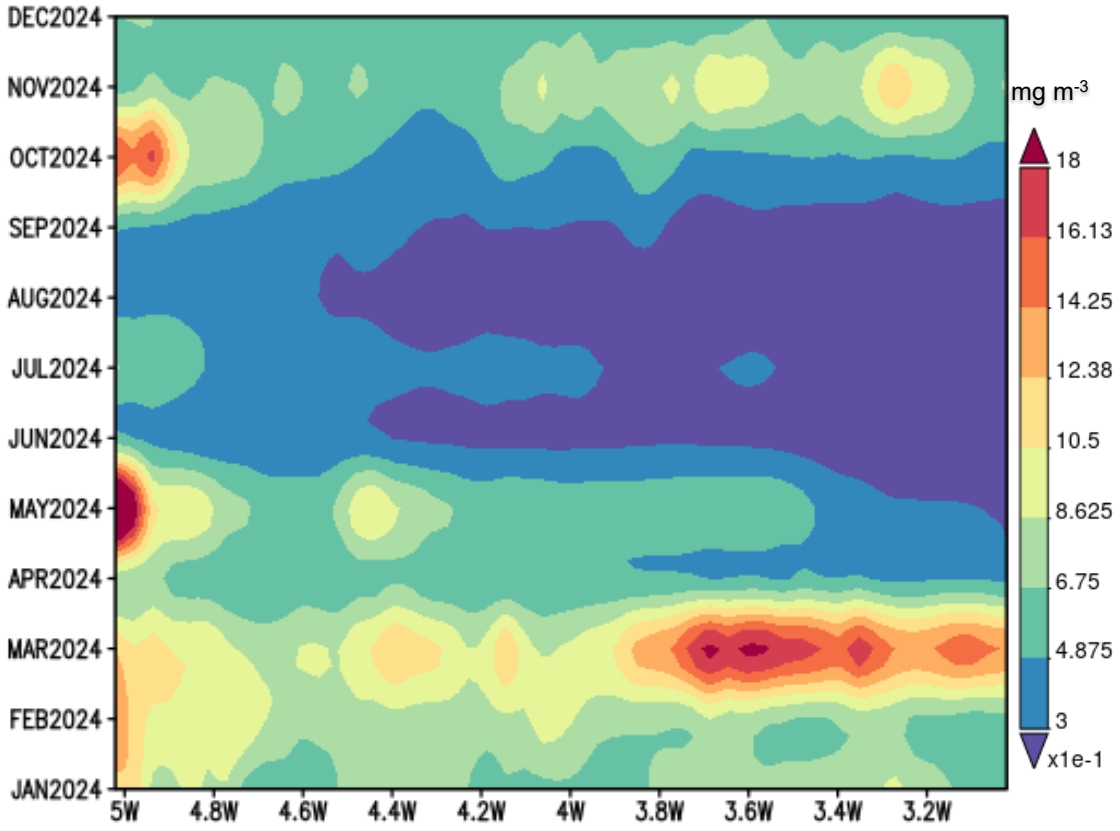

Figure 4: Analysis of monthly averaged chlorophyll concentrations (mg m^{-3}) for 2024 using Hovmöller latitude-averaged data. The investigated region is shown in Figure 1 as a yellow rectangle covering the area 5^0W, 35^0N to 3^0W, 37^0N.

The seasonal character of patchiness in chlorophyll concentrations is similarly expressed in the relationship between chlorophyll concentrations and sea surface temperature as is shown with scatter diagrams in Figure 5. Figure 5A shows that clusters appear throughout the year, but indicate that two

separate cluster appear with elevated chlorophyll concentrations when the data are grouped by seasons as in Figure 5B.

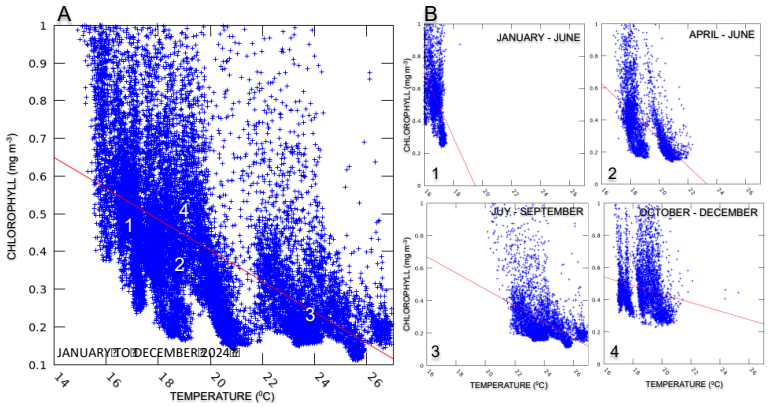

Figure 5: A: Scatter of temperature and chlorophyll concentrations for January to December 2024 that covers the region 5^{0}W, 35^{0}N to 3^{0}W, 37^{0}N as shown in Figure 1 as a yellow rectangle. B: Scatter diagrams of temperature and chlorophyll for 2024 by seasons. Note that the scales for temperature and chlorophyll concentrations are the same in all graphs.

Patchiness in chlorophyll concentrations is furthermore recognized in the Hovmöller longitude-averaged analysis of a section through the center of the gyre and is shown in Figure 6. There is a distinct difference in the development of temperature and chlorophyll concentration throughout the year demonstrating that the temperature goes through a rather smooth cycle, whereas the chlorophyll concentrations develop isolated patches at varying latitudes throughout the year.

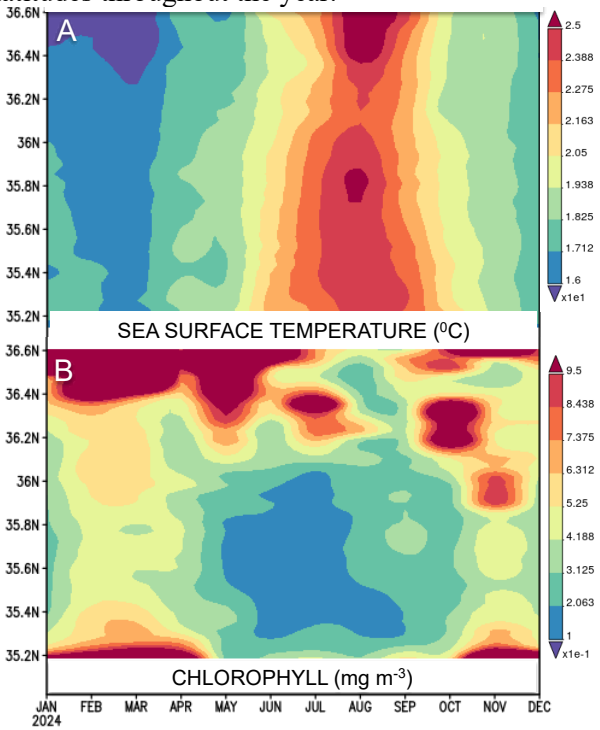

Figure 6: Hovmöller longitude-averaged analysis of temperature and chlorophyll for January to December 2024. The region is shown in Figure 1, numbered 2, as a white line. It covers a narrow stretch at 4^{0}36'W, 35^{0}N to 4^{0}30'W, 37^{0}N.

The upwelling region in the north has temperatures below 16^0C and high concentrations of chlorophyll that go to a minimum when the averaged monthly water temperature is greater than 25^0C. From January to July, the chlorophyll patches are an extension of the upwelling region and patches that are advected along the Atlantic Jet. At the start of the yearly cycle, two maxima of chlorophyll concentrations are observed in the northern upwelling region in February/March, and a second one is observed in May. The season June to October is marked by low concentrations throughout the region but light blooming is noted north in November, and blooming appears along the African coast.

Short-term fluctuations

As useful as monthly averaged data may be, they smooth out many of the details that may be of importance to the marine ecosystem, because changes are especially recognized in chlorophyll concentrations. Furthermore, chlorophyll concentrations are shown to appear to be more heterogeneous than temperature in their distribution. Especially, changing wind stress has an effect on surface conditions. Shown in Figure 7A, is a time series of surface wind speed that demonstrate that the wind speed can change vary quickly in the observed region with highest wind speed observed from February to April. Lowest wind speed was found during the summer but wind speed increased again towards the fall. Figure 7B shows an expanded view of wind speed for the season January to May when wind speed changed drastically and appeared as pulsing peaks.

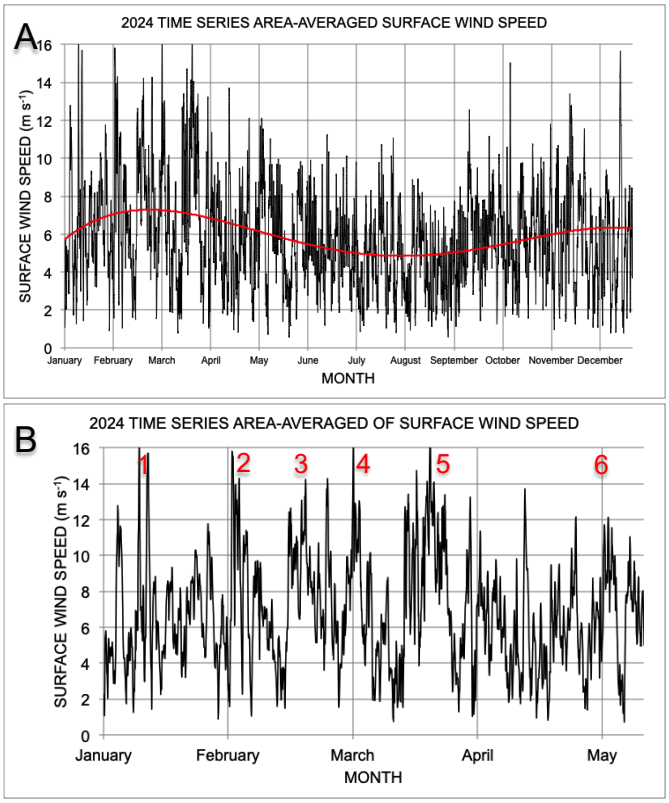

Figure 7 covers the area shown in Figure 1 as a small square. 7A: Averaged surface wind speed based on hourly 0.5 x 0.625 degree measurements (MERRA-2 Reanalysis). The red line shows a polynomial 3rd fit. Figure 7B shows the expanded x-axis for the season January to May with numbers in red showing the periodic maxima wind speed.

The pulsing nature of wind speed is explained as the cause for the sporadic blooming events that are typically observed during the spring of which a sequence of blooming event is shown in Figure 8. Blooming started in the upwelling region close to the Spanish coast and water with high chlorophyll content was advected along the outer periphery of the gyre, as is recognized in the images for 27 February and 2 March. A slight reduction in chlorophyll concentrations is observed on 15 March. However, on 3 April, blooming is again observed, although seven days later the concentration of chlorophyll is reduced in the whole gyre with minimum concentrations observed on 23 April. Another blooming event is observed on 3 May but lasts less than ten days. These observations indicate that major blooming events during the spring season may occur approximately every four weeks but have only a short life span in the neighborhood of days and would not be realized in monthly averaged data.

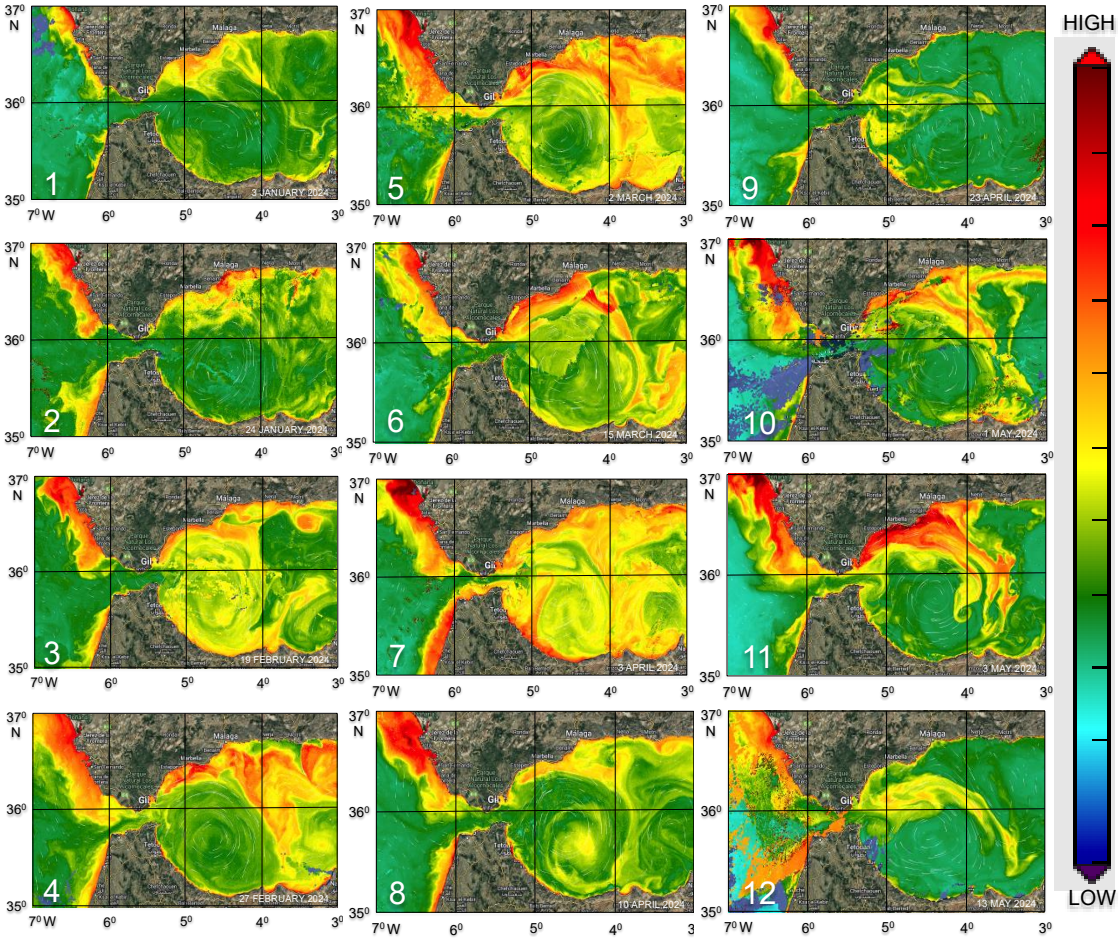

Figure 8: Cloudfree one-day coverage of chlorophyll concentrations from January to May 2024. The color bar provides an estimate of chlorophyll concentrations

Increasing surface temperature during the summer is associated with lower chlorophyll concentrations that reach a minimum in the center of the western gyre, and as Figure 8 indicates, elevated concentrations are mainly found along the periphery of the gyre, but in September, increasing chlorophyll concentrations are again observed and indicate that upwelling started in October along the Spanish coast.

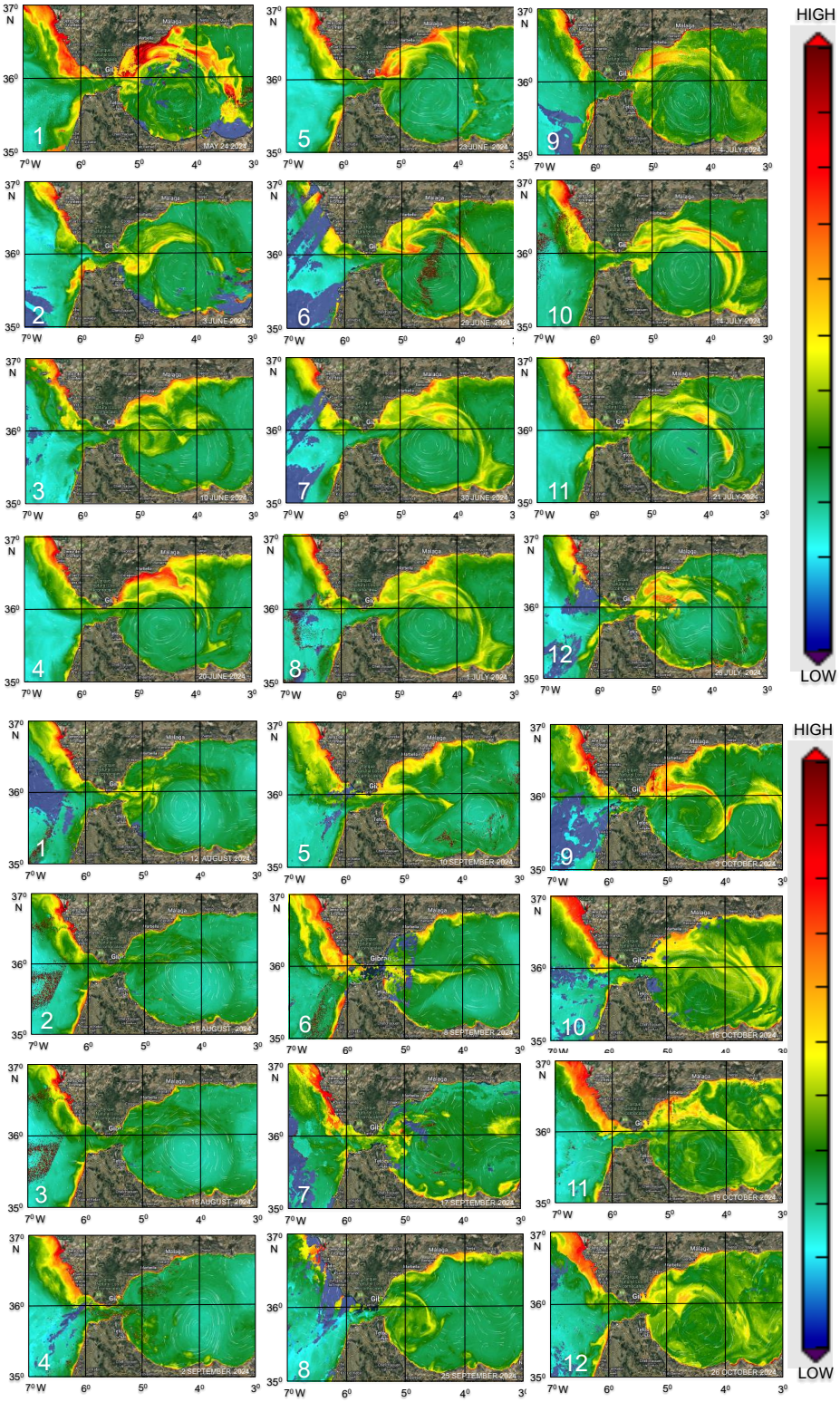

Figure 8 contd.: Cloudfree one-day coverage of chlorophyll concentrations from May to October 2024. The color bar provides an estimate of chlorophyll concentrations.

The fast changes in chlorophyll concentrations in the gyre demonstrate the problem to observe the temporal and spatial distribution of chlorophyll patches because cloud statistics limit close and continuous observations. However, occasionally, cloud-free images were acquired, and as shown in Figure 9, temporal and special changes of patches were recorded with an image sequence for March 2025.

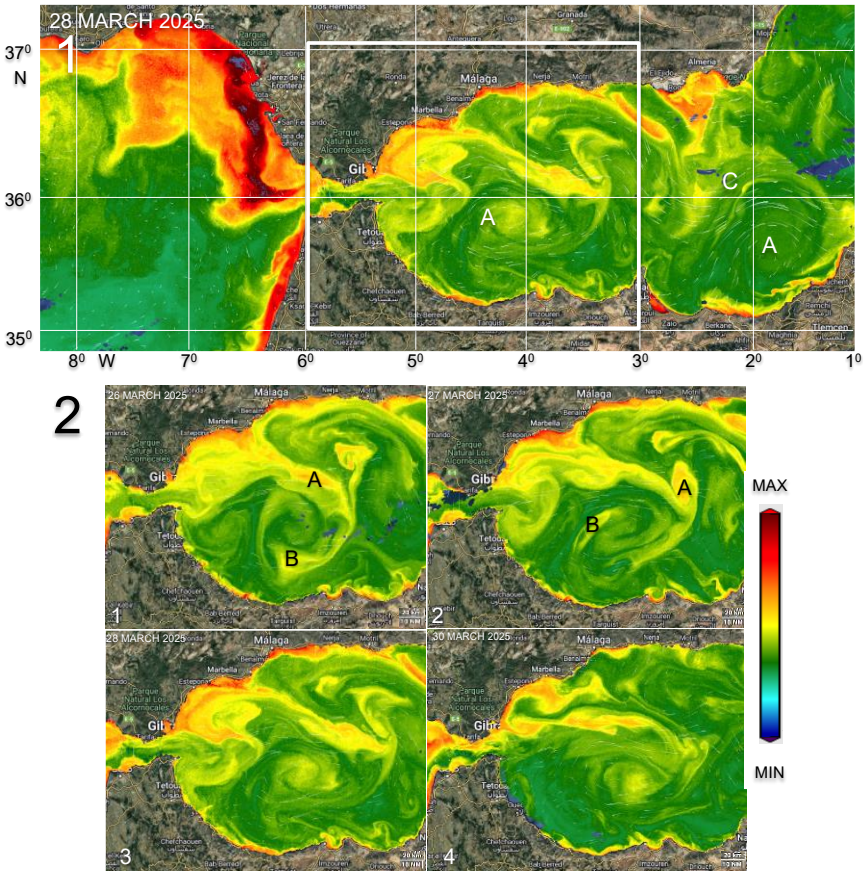

Figure 9: Cloudfree single-day coverage of chlorophyll concentrations from 26 March to 30 March 2025. Figure 9.1 is an enlarged coverage of the image shown in image 3, and it includes the white rectangle that locates the position of the images 1 to 4 in Figure 9.2. The color scale gives an approximation of chlorophyll concentrations.

Figure 9.1 covers the positions of two anticyclonic gyres and a smaller cyclonic gyre in the Alboran Sea on 26 March 2025. Figure 9.2 shows four images that were acquired over a time frame of four days and demonstrate the fast changes that may appear on the surface of the western Alboran gyre. A rough estimate on the velocity and displacement of chlorophyll patches can be derived from images of the gyre from 26 to 27 March, close to Marbella/ Sitio de Calahonda, at a time when blooming and its extension into the outer periphery were recognized. During this interval, two patches A and B were compared and their displacement estimated. Patch A moved at about 50km per day that corresponds to a speed of about 0.58 cm sec^{-1}, and a similar speed was estimated from patch B. The corresponding surface geostrophic current speed of the outer periphery of the gyre was recorded at 0.33 m s^{-1} on 26 March, but an increase of current speed of 0.49 m s^{-1} was recorded on 31 March. That chlorophyll patches are transported within the

current system and are advected from upwelled water along the boundary system can also be derived from the image series shown in Figure 10.

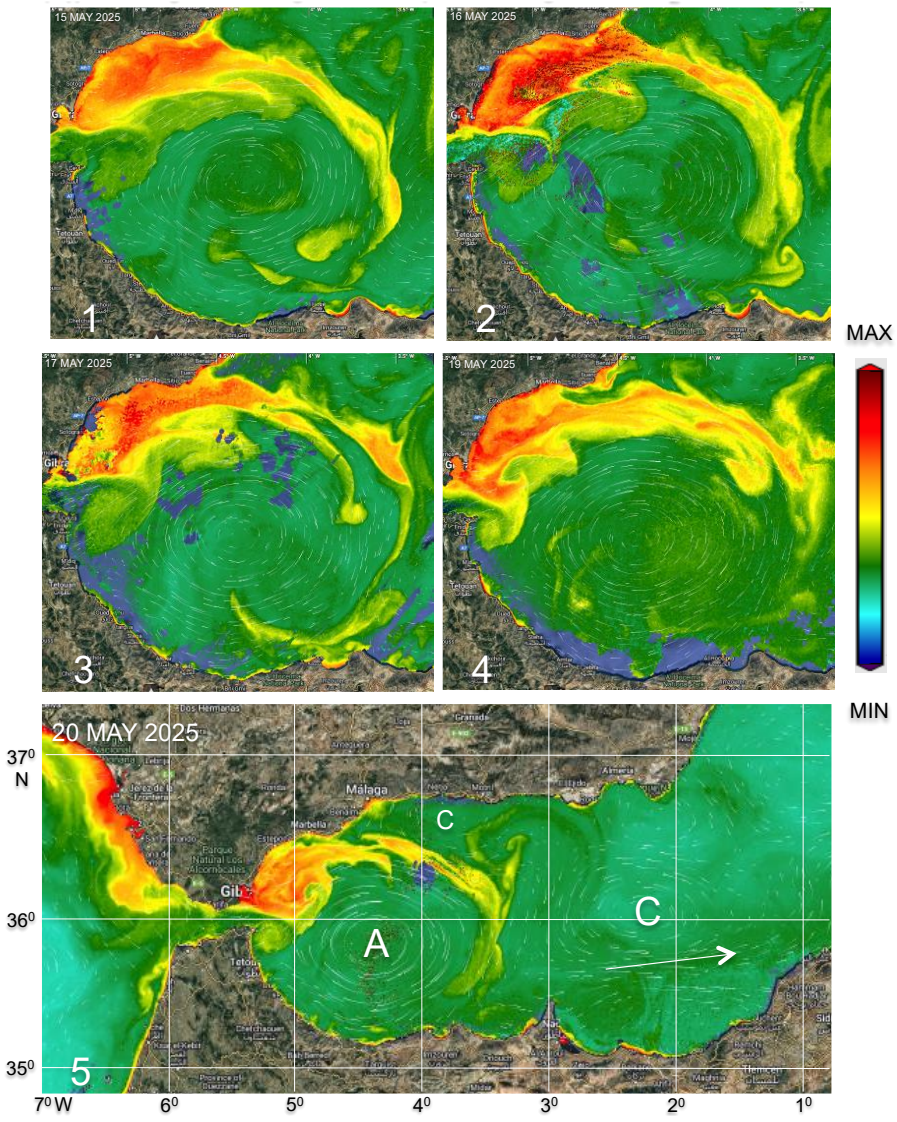

Figure 10: Comparison of chlorophyll patchiness and positions of the anticyclonic and cyclonic geostrophic surface currents from 15 May to 20 May 2025. Figure 10.5 shows a larger area of the Western Alboran Sea with the location of the anticyclonic and cyclonic gyres. A smaller anticyclonic gyre is located at the Spanish coast closed to Malaga. The arrow indicates the flow of the Atlantic Jet along the African Coast. The color scale gives an approximation of chlorophyll concentrations.

Patchy distribution in chlorophyll is generated by irregular transport from the northern upwelling system and biomass along the outer border of the gyre by the Atlantic Jet. Intense patch generation appears to be a seasonal mechanism because patches with high chlorophyll concentrations are observed especially during the second part of the year. Elevated chlorophyll concentrations along the outer periphery of the

gyre have been interpreted by Oguz *et al.* (2014) as a response to large vertical velocities of around 30 m d^{-1} that cause enhanced primary productivity and patch building of phytoplankton.
The observed complicated distribution structure in chlorophyll concentrations is shown with another example in Figure 11, where the general distribution pattern can be linked to the geostrophic surface circulation. Two large anticyclonic gyres are well established, and they border a cyclonic gyre in connection with the flow of the Atlantic Jet that surrounds the two anticyclonic gyres. Another strong cyclonic flow is located farther east, and two smaller gyres, cyclonic and anticyclonic, are located farther north.

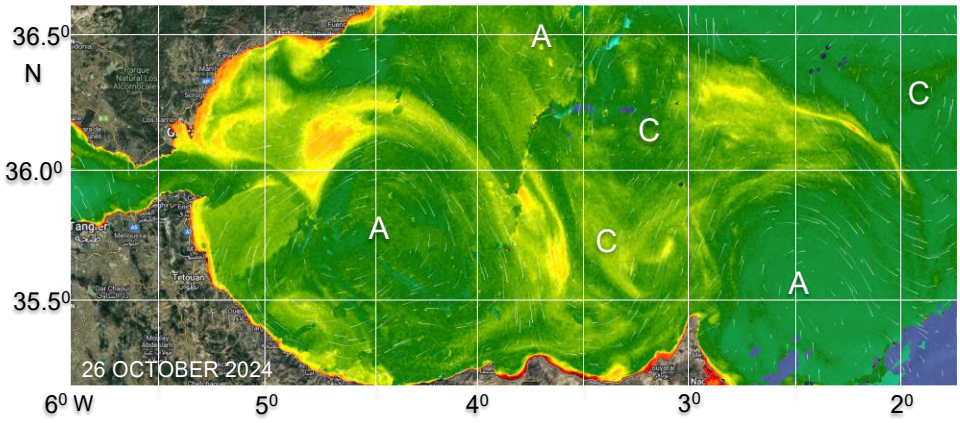

Figure 11: Comparison of chlorophyll distribution patterns and location of eddies based on geostrophic surface currents on 26 October 2024.

The geostrophic surface circulation show that the Alboran Sea is also occasionally subjected to extreme changes during which the western gyre may change its circulation from an anticyclonic to cyclonic mode within a very short time. Such an event was observed in 2024 when the western anticyclonic gyre changed from anticyclonic to cyclonic circulation within eighteen days. The cyclonic circulation was recognized at around 3⁰W on 30 October 2024. The anticyclonic gyre, while approaching the African coast, reduced its size, and by 3 November, two anticyclonic and three cyclonic gyres covered the western Alboran Sea. As shown in Figure 12, the anticyclonic gyre migrated east with its position close to the African coast. By 14 November, the circulation in the western Alboran Sea, close to the Strait of Gibraltar, was dominated by cyclonic circulation, but the anticyclonic gyre was still located adjacent to the African coast at around 3⁰30'W.

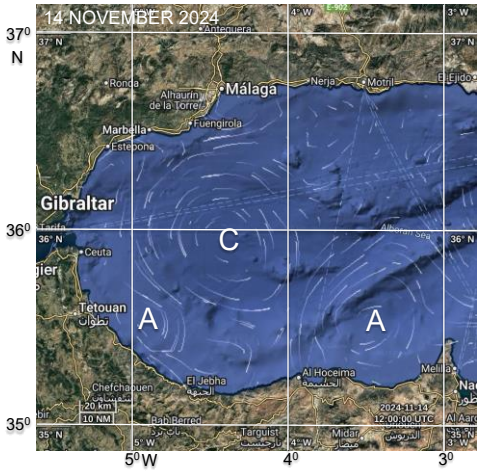

Figure 12: Eddy locations based on geostrophic surface currents on 14 November 2024.

The change from anticyclonic circulation seems to be too short for the biosphere to adapt completely to the different hydrographical conditions and to a new nutrient pool, because on 20 November, an anticyclonic circulation developed along the Moroccan coast as shown in Figure 13.1, and by 8 December was fully developed. Figure 13.3 demonstrates that by mid January the typical circulation in the Western Alboran Sea with two anticyclonic and one cyclonic gyre was reconstituted.

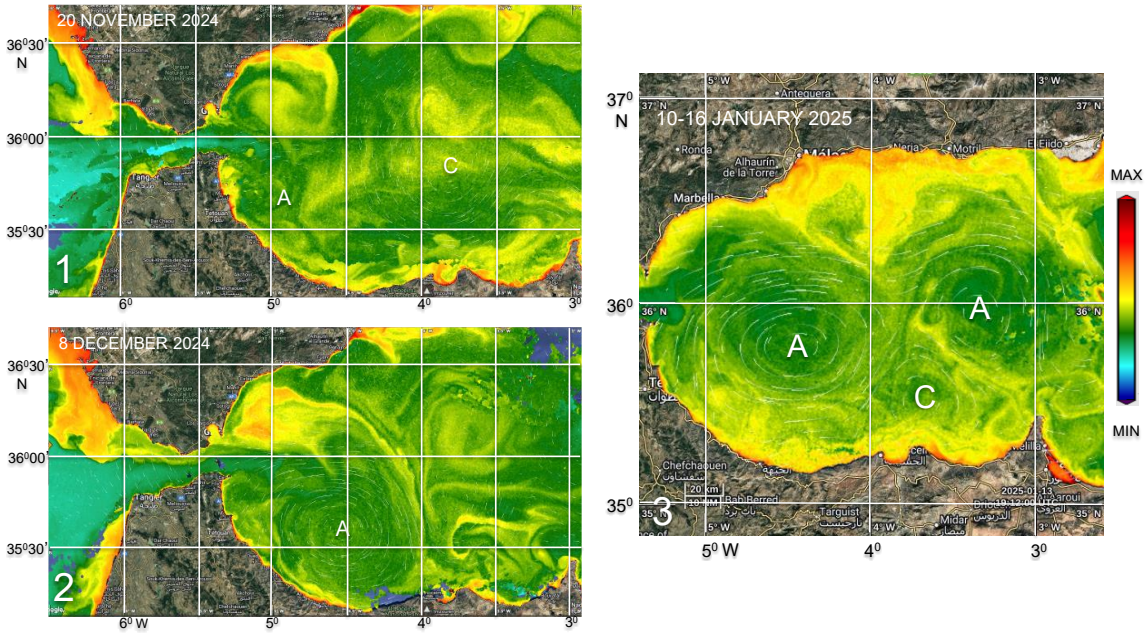

Figure 13: Images 13.1 and 13.2 show comparisons of chlorophyll distribution with the location of gyres identified by the geostrophic surface currents. Figure 13.1: Three-day chlorophyll concentration composite, 20 November 2024, with newly formed anticyclonic eddy A. Figure 13.2: Three-day composites of chlorophyll concentrations showing the progression of anticyclonic eddy A on 8 December 2024. Image 13.3: Fully developed anticyclonic and cyclonic eddies based on one-week composite of chlorophyll concentrations, January 2025.

CONCLUSIONS

The study showed that during the spring, blooming events may occur approximately every four weeks, but having only a short life span of a few days, they cannot be realized in monthly averaged data. The climatology data show that the central part of the gyre is characterized by low chlorophyll concentrations of <0.4 mg m^{-3}, but the concentrations are higher compared to those of the incoming Atlantic water that has less than 0.3 mg m^{-3}. The summer is associated with lower chlorophyll concentrations that reach a minimum in the center of the western gyre. The study revealed that patchiness in the chlorophyll distribution in the Alboran Sea is a common event and is a result of elevated chlorophyll concentrations that are transported from the northern upwelling system and additional biomass along the outer border of the gyre. Intense patch generation appears to be a seasonal mechanism as patches with high chlorophyll concentrations are observed especially during the first part of the year. Wind data indicate that following an increase of wind speed during the fall, blooming patches may be observed from February to April when highest wind speed occur. A rough estimate of the velocity and displacement of chlorophyll patches, derived by tracking patches, gave a speed of about 0.58 cm sec^{-1}. The western gyre may change its circulation from an anticyclonic to cyclonic mode within eighteen days but it seems to be that this

short period adds to the complicated surface distribution of chlorophyll.

ACKNOWLEDGEMENTS
The visualizations of data used in this study were produced with the Giovanni online data system, developed and maintained by NASA GES DISC. The MODIS mission scientists and associated NASA personnel are acknowledged for the production of the data used in this research effort. Acknowledged as well is the use of the ESA Ocean Virtual Laboratory and NASA Worldview for additional image retrieval.

REFERENCES
Acker JG and Leptoukh G (2007). Online analysis enhances use of NASA earth science data. *Eos, Transactions American Geophysical Union*, **88** (2) 14–17. https://doi.org/10.1029/2007EO020003 .
Bárcena MA, Flores JA, Sierro FJ, Perez-Folgado M, Fabres , Calafat A, Canals M (2004). Planktonic response to main oceanographic changes in the Alboran Sea (Western Mediterranean) as documented in sediment traps and surface sediments. *Marine Micropaleontology* **53** 423–445.
Boutov D, Peliz Á, Miranda PMA, Soares PMM, Cardoso RM, Prieto L, Ruiz J and García-Lafuente J (2014). Inter-annual variability and long term predictability of exchanges through the Strait of Gibraltar. *Global and Planetary Change* **114** 23-37.
Brett GJ, Pratt LJ, Rypina, II and Sánchez-Garrido JC. (2020). The Western Alboran Gyre: An analysis of its properties and its exchange with surrounding water. *Journal of Physical Oceanography* **50** 3379 – 3402.
Capó E, McWilliams JC, Mason E and Orfila A (2021). Intermittent frontogenesis in the Alboran Sea. *Journal of Physical Oceanography* **51** (5) 1417–1439. doi: 10.1175/JPO-D-20-0277.1
Cheney RE and Doblar RA (1982). Structure and variability of the Alboran Sea frontal system. *Journal of Geophysical Research* **87** 585–594. doi: 10.1029/JC087iC01p00585**.**
Cherif S, Doblas-Miranda E, Lionello P, Borrego C, Giorgi F, Iglesias A, Jebari S, Mahmoudi E, Moriondo M, Pringault O, Rilov G, Somot S, Tsikliras A, Vila M, Zittis G (2020). Drivers of change. In: *Climate and Environmental Change in the Mediterranean Basin – Current Situation and Risks for the Future. First Mediterranean Assessment Report* edited by Cramer W, Guiot J, Marini K (Union for the Mediterranean, Plan Bleu, UNEP/MAP, Marseille, France) 59-180. doi:10.5281/zenodo.7100601.
Esposito G, Berta M, Centurioni L, Johnston TMS, Lodise J, Özgökmen T, Poulain P-M and Griffa A (2021). Submesoscale Vorticity and Divergence in the Alboran Sea: Scale and Depth Dependence. *Frontiers in Marine. Science* 8:678304. doi: 10.3389/fmars.2021.678304 **Garćia-Gorriz E, Carr ME (2001)**. Physical control of phytoplankton distributions in the Alboran Sea: a numerical and satellite approach. *Journal of Geophysical Research* **106** 16795 – 16805.
Garcıá-Lafuente J, BruquePozas E. Sánchez-Garrido JC, Sannino G and Sammartino S (2013). The interface mixing layer and the tidal dynamics at the Eastern part of the strait of Gibraltar. *Journal of Marine Systems* 117–118. doi: 10.1016/ j.jmarsys.2013.02.014.
Huertas IE, Rıós AF, Garcıá-Lafuente J, Navarro G, Makaoui A, Sánchez-Roman A, et al. (2012). Atlantic Forcing of the Mediterranean oligotrophy. *Global Biogeochemistry* Cy. 26 GB2022. doi: 10.1029/2011GB004167.
LaViolette PE (1984). The advection of cyclonic submesoscale thermal features in the Alboran Sea. *Journal of Physical Oceanography* **14** (3) 550–565. doi: 10.1175/1520-0485(1984)014<0550:TAOSTF>2.0.CO;2.
LaViolette PE and Lacombe H (1988). Tidal-induced pulses in the flow through the Strait of Gibraltar. *Oceanologica Acta*, *Océanographie pélagique méditerranéenne*, edited by Minas HJ and Nival P 13-27.
Maćias D, Garcia-Gorriz E, Stips A. (2016). The seasonal cycle of the Atlantic Jet dynamics in the Alboran Sea: direct atmospheric forcing versus Mediterranean thermohaline circulation. *Ocean Dynamics* **66** 137–151. DOI 10.1007/s10236-015-0914-y.

Moran XAG and Estrada M (2001). Short-term variability of photosynthetic parameters and particulate and dissolved primary production in the Alboran Sea (SW Mediterranean). *Marine Ecology Progress* Series 212 53–67. doi:0.3354/meps212053

Oguz T, Macıás D, Garcıá-Lafuente J, Pascual A and Tintoré J (2014). Fueling plankton production by a meandering frontal jet: A case study for the Alboran Sea (Western Mediterranean). *PloS One* 9 (11) e111482. doi: 10.1371/ journal.pone.0111482.

Parrilla G and Kinder TH (1987). The Physical Oceanography of the Alboran Sea. Naval Ocean Research and Development Activity. NORDA Report 184 26 pp.

Ramırez T, Muñoz M, Reul A, Garcıá-Martinez C, Moya F, Vargas-Yáñez,M, et al. (2021). The biogeochemical context of marine planktonic ecosystems. In: *Alboran Sea – ecosystems and marine resources*, edited by Báez JC, Vázquez JT, Caminas JA and Malouli M (Springer Nature Switzerland AG).

Renault L, Oguz T, Pascual A, Vizoso G, and Tintore J (2012). Surface circulation in the Alborán Sea (western Mediterranean) inferred from remotely sensed data, *Journal of Geophysical Research* 117 C08009. doi:10.1029/2011JC007659**.**

Reul A, Muñoz M and Bautista B (2015). Spatio-temporal variability in the NW-Alboran Sea upwelling area and derived estimates of nitrate upwelling and POC downwelling. In: *Volumen de comunicaciones presentadas en el Simposio Sobre El Margen Ibérico Atlántico*, Publisher: Instituto Español de Oceanografía, Ediciones Sia Graf 221 – 224**.**

Sánchez-Garrido JC, Lafuente JG, Fanjul EÁ, García Sotillo M, de los Santos FJ (2013). What does cause the collapse of the Western Alboran Gyre? Results of an operational ocean model. *Progress in Oceanography* 116, 142–153.

Sánchez-Garrido JC and Nadal I (2022). The Alboran Sea circulation and its biological response: A review. *Frontiers in Marine Science* 9:933390. doi: 10.3389/fmars.2022.933390.

Sánchez-Garrido JC, Naranjo C. Maćias D, Garcia-Lafuente J and Oguz T (2015). Modeling the impact of tidal flow on the biological productivity of the Alboran Sea. *Journal of Geophysical Research*, *Ocean* **120** (11) 7329-7345. doi: 10.1002, 2015JC010885.

Sarhan T, García-Lafuente, Vargas JM and F. Plaza F (2000) Upwelling mechanisms in the northwestern Alboran Sea, *Journal of Marine Systems* **23**, 317–331, doi:10.1016/S0924-7963(99)00068-8

Vargas-Yáñez M, Garcıá-Martinez M, Moya F, Balbıń R and López-Jurado J. (2021). The oceanographic and climatic context. In *Alboran Sea – Ecosystems and Marine Resources*, Chapter 4, edited by Báez JC, Vázquez JT, Caminas JA and Malouli M (Springer Nature Switzerland AG), ISBN: . doi: 10.1007/978-3-030- 65516-7_4.

Vargas-Yáñez M, Plaza F, Garcıá-Lafuente J, Sarhan T, Vargas JM and Vélez-Belchi P (2002). About the seasonal variability of the Alboran Sea circulation. *Journal of Marine Systems* **35** (3–4),229–248. doi: 10.1016/S0924-7963(02)00128-8.

Vélez-Belchí P, Vargas-Yáñez M and Tintoré J (2005). Observation of a Western alboran gyre migration. *Progress in Oceanography* 66 190–210. doi: 10.1016/ j.pocean.2004.09.006.